Three-body vs. dineutron approach to two-neutron radiative capture in ⁶He

Physics Letters B 807 (2020) 135557

Contents lists available at ScienceDirect

Physics Letters B

www.elsevier.com/locate/physletb

Three-body vs. dineutron approach to two-neutron radiative capture in ^{6}He

L.V. Grigorenko [a,b,c,*], N.B. Shulgina [c,d], M.V. Zhukov [e]

[a] Flerov Laboratory of Nuclear Reactions, JINR, 141980 Dubna, Russia
[b] National Research Nuclear University "MEPhI", Kashirskoye shosse 31, 115409 Moscow, Russia
[c] National Research Centre "Kurchatov Institute", Kurchatov sq. 1, 123182 Moscow, Russia
[d] Bogoliubov Laboratory of Theoretical Physics, JINR, 141980 Dubna, Russia
[e] Department of Physics, Chalmers University of Technology, S-41296 Göteborg, Sweden

ARTICLE INFO

Article history:
Received 27 March 2020
Received in revised form 3 May 2020
Accepted 10 June 2020
Available online 16 June 2020
Editor: W. Haxton

Keywords:
Two-neutron nonresonant radiative capture reaction
Soft dipole mode
Neutron halo
Three-body hyperspherical harmonics method
Dynamical dineutron model

ABSTRACT

The low-energy behavior of the strength function for the 1^- soft dipole excitation in ^{6}He is studied theoretically. Use of very large basis sizes and well-grounded extrapolation procedures allows to move to energies as small as 1 keV, at which the low-energy asymptotic behavior of the E1 strength function seems to be achieved. It is found that the low-energy behavior of the strength function is well described in the effective three-body "dynamical dineutron model". The astrophysical rate for the α+n+$n \to ^6$He+γ is calculated. Comparison with the previous calculations is performed.

1. Introduction

The astrophysical radiative capture rates $\langle \sigma_{\mathrm{capt},\gamma} v \rangle$ are prime ingredients of the network nucleosynthesis calculations in the thermalized stellar environment. Some rates may be directly derived from experimental data. Some of them require sophisticated theoretical calculations and development of the adequate theoretical methods is essential in such cases.

The ability to reproduce in one theoretical calculation the behavior of the electromagnetic strength function *simultaneously* at intermediate energies $E_T \sim 0.5 - 5$ MeV and at very low energies $E_T \lesssim 0.1 - 0.5$ MeV is crucial for determination of the low-temperature astrophysical capture rates based on experimental data (E_T is energy relative to the corresponding breakup threshold). The common idea is to measure the electromagnetic cross section at reasonably high energy (where it is relatively high) and then to extrapolate it to low energy theoretically, see Fig. 1. For two-body radiative captures $A_1 + A_2 \to A_{12} + \gamma$ this extrapolation is quite straightforward, which can be illustrated by analytical R-matrix type expression

$$\frac{d\sigma_{A_1A_2,\gamma}}{dE_T} \sim \frac{\Gamma(E_T)}{(E_T - E_r)^2 + \Gamma^2_{\mathrm{tot}}/4}\,, \qquad \Gamma(E_T) \sim P_l(E_T)\,, \tag{1}$$

where the low energy asymptotic behavior is defined by the penetrability function P_l with definite angular momentum l. Obviously, this expression is valid for resonant radiative capture. For nonresonant captures the direct calculation of the electromagnetic strength function (SF) $dB_{\pi\lambda}/dE_T$ of relevant multipolarity $\pi\lambda$ is required. However, qualitative (especially, the low-energy) behavior of this SF is still mainly determined by the penetrability function P_l.

For the three-body radiative captures the situation is far not that straightforward. Since the classical paper [1] and till the modern compilation [2] the semiclassical expression for *two-step* capture is commonly used for determination of the three-body rates $A_1 + A_2 + A_3 \to A_{123} + \gamma$,

$$\langle \sigma_{A_1A_2A_3,\gamma} v \rangle = \sum_i \frac{\langle \sigma_{A_1A_2,(A_1A_2)} v \rangle_i}{\Gamma_{(A_1A_2),i}} \langle \sigma_{(A_1A_2)A_3,\gamma} v \rangle_i\,, \tag{2}$$

* Corresponding author.
E-mail address: lgrigorenko@yandex.ru (L.V. Grigorenko).

https://doi.org/10.1016/j.physletb.2020.135557

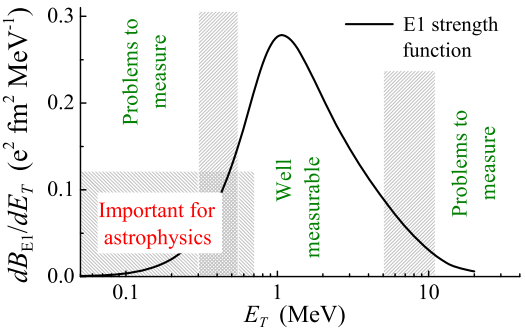

Fig. 1. Schematic view of the soft dipole strength functions and energy ranges available for measurements and important for astrophysics.

where i is the number of the intermediate resonance populated at the first step of capture into (A_1A_2) subsystem. This expression is obtained from the rate equations for balance of three particles $(A_1A_2A_3)$

$$\begin{aligned}\dot{Y}^{(i)}_{(A_1A_2)} &= N_A\,\rho\,\left\langle\sigma_{A_1A_2,(A_1A_2)}v\right\rangle_i\,Y_{A_1}Y_{A_2}\\ &\quad-\Gamma_{(A_1A_2),i}\,Y^{(i)}_{(A_1A_2)}\,,\\ \dot{Y}_{(A_1A_2A_3)} &= \sum_i N_A\,\rho\,\left\langle\sigma_{(A_1A_2)A_2,\gamma}v\right\rangle_i\,Y^{(i)}_{(A_1A_2)}Y_{A_3}\,,\end{aligned}\tag{3}$$

where $Y^{(i)}_A$ are abundances of the species A in the state i, ρ is the density of the stellar media and N_A is Avogadro constant. Equation (2) arises under the assumption of thermodynamic equilibrium for the intermediate resonant states: $\dot{Y}^{(i)}_{(A_1A_2)}\equiv 0$. Thus, the ratio

$$\left\langle\sigma_{A_1A_2,(A_1A_2)}\,v\right\rangle_i/\Gamma_{(A_1A_2),i}$$

determines the classical concentration of the subsystem (A_1A_2) in the resonant state number i in stellar media. Being essentially classical, the Eq. (2) does not hold for a number of genuine quantum-mechanical situations. An example of such a situation is the direct $2p$ radiative capture, which is the reciprocal process of $2p$ radioactive decay [3].

To formally generalize Eq. (2) for nonresonant capture rates [1,2] it is implicitly assumed that the ratio

$$\frac{\sigma_{A_1A_2,(A_1A_2)}(E)\,v(E)}{\Gamma_{(A_1A_2)}(E)}\,,\tag{4}$$

can be interpreted as the classical concentration of composite subsystems A_1+A_2 at any given energy E smaller than any resonance energy in the system. It was found that although this idea *qualitatively* looks quite reasonable, the direct three-particle calculations can reveal important *quantitative* effects [3–6].

As a rule, the prevailing contribution to three-body nonresonant capture in a wide temperature range gives the dipole transition E1. Thus, the problem of three-body rates is connected with studies of soft dipole excitations (or soft dipole mode, SDM) in halo systems. In the papers [4–6] we focused on the $2p$ captures, studied by the example of the ^{15}O+p+$p\to{}^{17}$Ne+γ reaction. It was found that semisequential dynamics (governed by the lowest resonances in the core+p subsystem) is essential for the low-energy behavior of the E1 SF determining the rate for this reaction. In this work we studied the $2n$ captures for the case of the α+n+$n\to{}^6$He+γ reaction. We find that for the $2n$ captures the situation is qualitatively different: the low-energy behavior of the E1 SF here is governed by the dynamics of the virtual state (spin-singlet s-wave scattering) in the n-n channel.

The astrophysical site, where α+n+$n\to{}^6$He+γ reaction (and analogous two-neutron captures) may become important is the r-process of nucleosynthesis in neutron-rich stellar media in conditions of high density, which makes possible three-body radiative captures. At the same time, the temperature should not be too high to avoid the inverse process of the photodisintegration. Several scenarios were suggested by astrophysicists: (i) the neutrino-heated hot bubble between the nascent neutron star and the overlying stellar mantle of a type-II supernova, (ii) the shock ejection of neutronized material via supernovae, (iii) merging neutron stars. Environment conditions such as temperatures and densities for these scenarios are quite different. For details see Ref. [7,8, and Refs. therein]. Calculations for specific scenarios may be the subject of separate studies.

There is a big difference in theoretical estimates of the $2n$ capture rates for the α+n+$n\to{}^6$He+γ reaction: the results of papers [7–12] are highly inconsistent with each other. Important motivation of this work is also to get out of this uncertain situation.

2. Low-energy convergence of the E1 SF

The soft dipole excitation in ^{6}He was studied in details in the recent paper [13]. For studies of E1 excitation the inhomogeneous three-body Schrödinger equation is solved

$$\begin{aligned}&\left[\hat{H}_3+\tilde{V}_3(\rho)-E_T\right]\Psi^{JM(+)}_{M_im}=\mathcal{O}_{\mathrm{E1},m}\Psi^{J_iM_i}_{\mathrm{gs}}\,,\\ &\hat{H}_3=\hat{T}_3+V_{cn_1}(\mathbf{r}_{cn_1})+V_{cn_2}(\mathbf{r}_{cn_2})+V_{n_1n_2}(\mathbf{r}_{n_1n_2})\,,\end{aligned}\tag{5}$$

providing the WF $\Psi^{JM(+)}_{M_im}$ with pure outgoing wave asymptotics. The E1 transition operator has the following form

$$\mathcal{O}_{\mathrm{E1},m}=e\sum_{i=1,3}Z_i\,r_i\,Y_{1m}(\hat{r}_i)\,,$$

and $\Psi^{J_iM_i}_{\mathrm{gs}}$ is the ^{6}He g.s. WF. The three-body potential $\tilde{V}_3$ provides phenomenological way to take into account the many-body effects in three-cluster system, which are beyond the three-cluster approximation. The possible effect of this potential was shown to be not very important in [13] and we neglect it in this work as well. The E1 strength function is then expressed via outgoing flux j associated with the WF $\Psi^{JM(+)}_{M_im}$:

$$\frac{dB_{\mathrm{E1}}}{dE_T}=\frac{1}{2\pi}\sum_J\frac{2J+1}{2J_i+1}\,j_J\,.\tag{6}$$

The hyperspherical expansion of the continuum WF

$$\Psi^{JM(+)}_{M_im}=C^{JM}_{J_iM_i1m}\,\rho^{-5/2}\sum_{K\gamma}\chi^{(+)}_{JK\gamma}(\varkappa\rho)\,\mathcal{J}^{JM}_{K\gamma}(\Omega_\rho)\,,\tag{7}$$

is truncated in our calculations by the maximum value of the generalized angular momentum $K=K_{\mathrm{FR}}$. However, also the effective three-body potentials are used when solving Eq. (5), which are obtained by adiabatic procedure (so called "Feshbach reduction") and this procedure allows to use much larger effective basis sizes $K=K_{\max}$.

It was shown in [13] that the increasingly large size of hyperspherical basis is needed to obtain converged E1 SF when moving to lower energies, see Figs. 3 and 4 of [13]. Visually converged E1 SF was obtained in the whole energy range. However, if we investigate the extreme low-energy part of the SF (also the range, important for astrophysical calculations) we can find that the problem persists. One may see in Fig. 2 that even in the largest-basis calculations of [13] with $K_{\max}=101$ the SF is converged down to $E_T\sim 60-80$ keV. At lower energies (e.g. at $E_T=1$ keV), the curves corresponding to $K_{\max}=101$, 91, 81 are nearly equidistant indicating very slow convergence at maximum $K_{\max}$ achieved in the calculations.

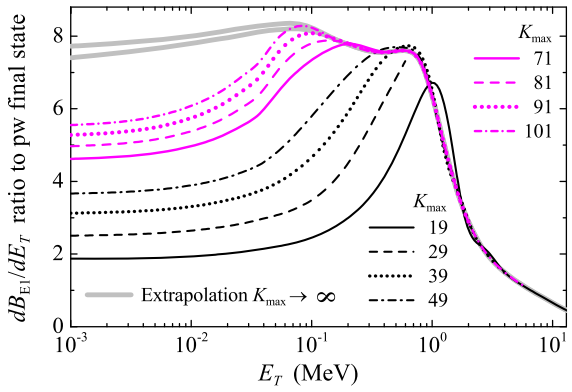

Fig. 2. Low-energy ratio of the E1 SF calculated with full three-body Hamiltonian to that obtained in the "no FSI" approximation (plane wave final state is used). Curves correspond to different sizes K_{max} of the hyperspherical basis. Gray curves correspond to exponential extrapolation to infinite basis, see Fig. 3 (upper and lower boundaries, defined by the extrapolation uncertainty). See also Fig. 4 of Ref. [13].

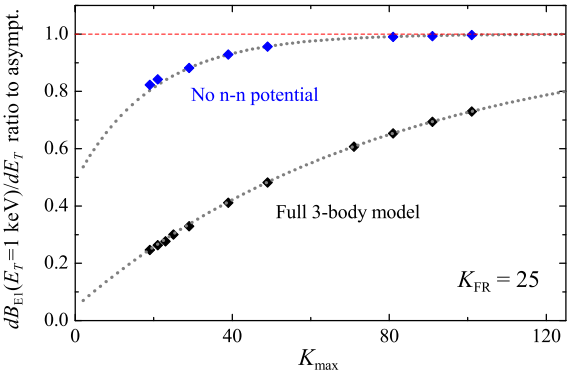

Fig. 3. Example of the convergence of the E1 SF for $E_T = 1$ keV calculated in full three-body model and with n-n FSI switched off (diamonds). Dotted curves show exponential extrapolation to infinite basis by Eq. (8).

What to do in this situation? It can be seen in Fig. 3 that the convergence over K_{max} has perfectly exponential character

$$\frac{dB_{E_1}(E_T, K_{max})}{dE_T} = \frac{dB_{E_1}(E_T, \infty)}{dE_T} - c_1 \exp\left(-\frac{K_{max}}{c_2}\right), \qquad (8)$$

in a broad range of K_{max} values from about 35 to 101. The exponential convergence character is known for *binding energies* of three-body systems with certain "good" two-body potentials (non-singular and short-range) [14]. The exponential convergence character of *three-body widths* was numerically demonstrated in Refs. [15–19]. So, analogous observation for low-energy E1 SF is not completely unexpected. The exponential convergence character in Fig. 3 means that enormous basis sizes are needed for complete convergence at low E_T values: at $E_T = 1$ keV the 95% convergence would be achieved at $K_{max} \sim 250$. Direct calculation is thus not an option in such situation.

Where is the source of the convergence problem? We have found in [13] that the low energy convergence of the SF is much faster if the n-n interaction is switched off. The same calculations performed for such a "truncated" Hamiltonian in the low-energy domain indicate that the convergence issue is not severe in this case, see Fig. 4. The calculations with the "no n-n FSI" three-body Hamiltonian are fully converged (the 95% convergence is achieved with $K_{max} \sim 45$, see Fig. 3). However, this approximation provides drastically smaller (~ 9 times) values of the E1 SF in the low-energy domain, which shows that the n-n FSI is essential for the question.

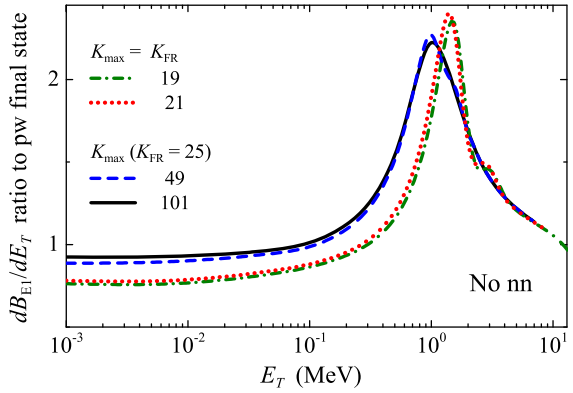

Fig. 4. The same as Fig. 2, but for "no n-n FSI" three-body Hamiltonian. See also Fig. 4 of Ref. [13].

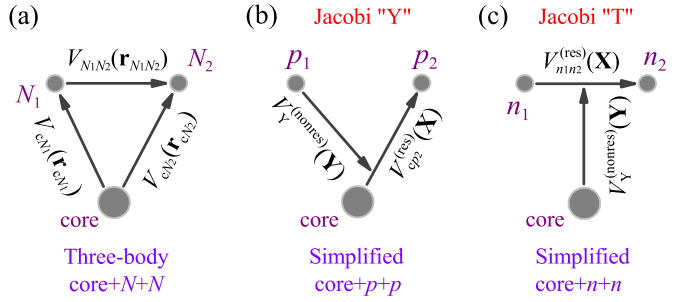

Fig. 5. Simplification of the calculation scheme for SDM in the three-body case. (a) Initial complete 3-body Hamiltonian. (b) For core+p+p system the dynamical domination of resonances in the core-p subsystem motivates the use of simplified Hamiltonian in the "Y" Jacobi system. (c) For core+n+n system the dynamical domination of the n-n FSI motivates the use of simplified Hamiltonian in the "T" Jacobi system.

3. Dynamical dineutron model of SDM

Because the behavior of E1 SF in ^{6}He is so sensitive to virtual state in the spin-singlet n-n channel, then maybe a good approximation to it can be obtained by taking into account *only* the dynamics of the "dineutron". This can be done applying the formalism developed in [4,6] for studies of SDM excitations in ^{17}Ne, but in the "T" Jacobi system, see Fig. 5. What we get in this case can be called "dynamic dineutron model". Analogous model we have already applied for qualitative studies of two-neutron emission in dineutron approximation [20].

The idea of the method is that for E1 excitation studies instead of solving the three-body Schrödinger equation (5) with Hamiltonian $\hat{H}_3$ we introduce the simplified Hamiltonian

$$\hat{H}'_3 = \hat{T}_3 + V_y(\mathbf{Y}) + V_{n_1n_2}(\mathbf{X}), \qquad (9)$$

which factorize the degrees of freedom in the "T" Jacobi system, see Fig. 5. The latter Hamiltonian allows exact semianalytical solution, since it has Green's function of a simple analytical form, which (schematically) looks like

$$G^{(+)}_{E_T}(\mathbf{XY}, \mathbf{X'Y'}) = \frac{1}{2\pi i}\int dE_x G^{(+)}_{E_x}(\mathbf{X}, \mathbf{X'}) G^{(+)}_{E_T - E_x}(\mathbf{Y}, \mathbf{Y'}),$$

where $G^{(+)}_{E_x}(\mathbf{X}, \mathbf{X'})$ and $G^{(+)}_{E_T-E_x}(\mathbf{Y}, \mathbf{Y'})$ are ordinary two-body Green's functions of the X and Y subsystems. This approach can be justified if the interactions $V_{cn_1}(\mathbf{r}_{cn_1})$ and $V_{cn_2}(\mathbf{r}_{cn_2})$ in (5) are not of a prime importance for the system dynamics and can be replaced with one effective interaction $V_y(\mathbf{Y})$. It can be seen in Fig. 5 that both in two-proton case (b) and in two-neutron case (c) the

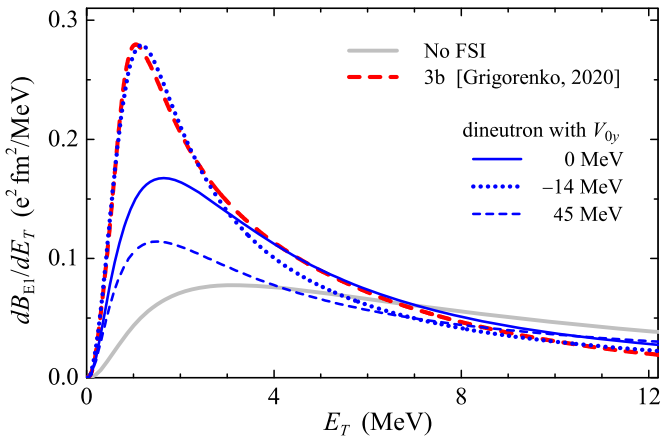

Fig. 6. Comparison of the E1 strength functions calculated in full three-body model (Grigorenko, 2020: [13]), in "no FSI" approximation, and in different dineutron model settings.

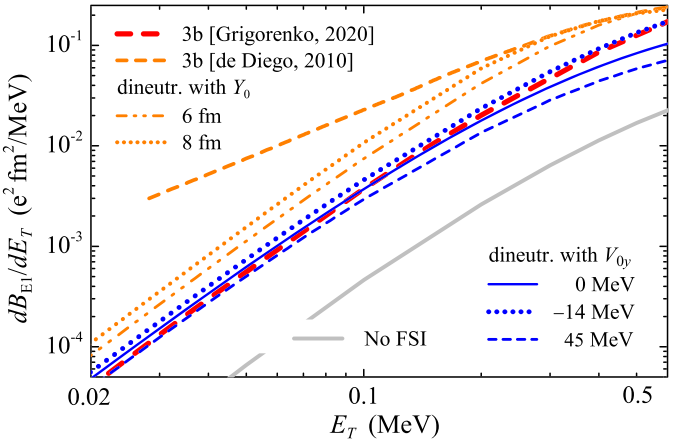

Fig. 7. Comparison of the low-energy asymptotics of the E1 strength functions calculated in full three-body model (Grigorenko, 2020: [13]), in "No FSI" approximation, in different dineutron model settings, and in paper (de Diego, 2010: [10]).

dynamically important (in both cases resonant) interaction is associated with X coordinate, while de-facto insignificant interactions are "hidden" in the effective interaction V_y depending only on the Y coordinate. For technical details of the three-body method and dineutron approximation, see Refs. [13,20].

The calculations of E1 SF within dynamical dineutron model are shown in Fig. 6. Three test interactions in the Y subsystem have the Gaussian formfactors

$$V_y(Y) = V_{0y}\,\exp[-(Y/Y_0)^2]\,,$$

with $Y_0 = 3$ fm, acting in p-wave only. They are: (i) no interaction $V_{0y} = 0$ (leads to plane wave over Y coordinate), (ii) attraction with $V_{0y} = -14$ MeV, and (iii) repulsion with $V_{0y} = 45$ MeV. Attractive interaction was fitted to reproduce the profile of the three-body E1 strength function in a broad energy range. However, if we turn to low-energy behavior of the E1 SF in Fig. 7, then we see that the best match with calculated low-energy behavior of a three-body SF is obtained with repulsive V_y potential. The "trivial" assumption of the absence of interaction $V_{0y} = 0$ in Y subsystem leads to overall good agreement with the three-body SF. In any case a comparison of attractive and strongly repulsive interactions shows a mismatch of only $\lesssim 50\%$ in the low-energy region. Therefore, the uncertainty associated with the "unphysical" interaction V_y is not large in the asymptotic region anyhow, although it changes drastically the profile of the E1 SF at higher energies.

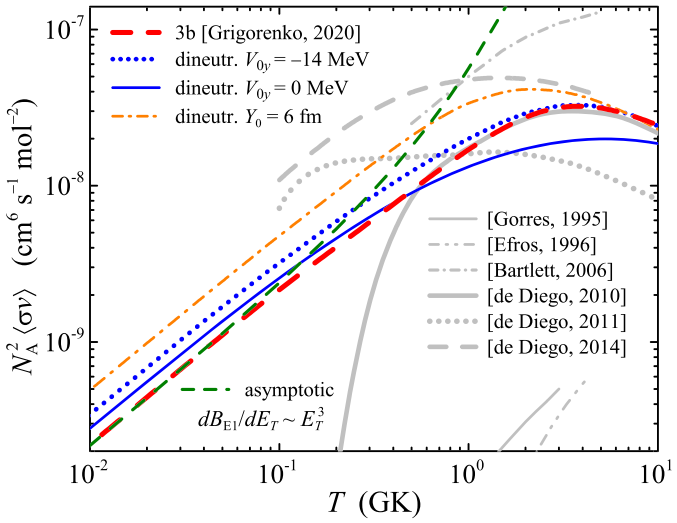

Fig. 8. Three-body astrophysical radiative capture rates for the α+n+$n \to {}^6$He+γ reaction obtained with different E1 SFs in this work (colored curves) and in the other models (gray curves) in Refs. (Görres, 1995: [9]), (Efros, 1996: [7]), (Bartlett, 2006: [8]), (de Diego, 2010: [10]), (de Diego, 2011: [11]), (de Diego, 2014: [12]).

The nearly linear behavior of the E1 SFs in the left part of log-scale Fig. 7 indicates that the correct low-energy asymptotic behavior

$$dB_{E_1}(E_T)/dE_T \sim E_T^3\,, \tag{10}$$

is almost achieved.

4. Three-body capture rate

The E1 nonresonant astrophysical radiative capture rate for the three-body reactions is given by the expression

$$\langle\sigma_{A_1A_2A_3,\gamma}\,v\rangle = \left(\frac{\sum A_i}{\prod A_i}\right)^{3/2}\left(\frac{2\pi}{mkT}\right)^3\frac{2(2J_f+1)}{\prod(2J_i+1)} \times\int dE_T\,\frac{16\pi}{9}\,E_\gamma^3\,\frac{dB_{E1}(E_T)}{dE_T}\exp\left[-\frac{E_T}{kT}\right], \tag{11}$$

where $E_\gamma = E_T + E_b$ ($E_b = 0.973$ MeV for ^{6}He) and J_i are the spins of incident clusters, while J_f is the spin of the bound final state (0^+ in the ^{6}He case). Note that the E1 strength function dB_{E1}/dE_T in Eq. (11) is the strength function for the reciprocal process of ^{6}He E1 EM dissociation.

The two-neutron capture rates calculated with SFs discussed above are shown in Fig. 8. The most trivial dineutron model result with $V_{0y} = 0$ has a good overall agreement with the three-body result (the deviation is never more than $\sim 50\%$). The temperature region from 1 to 10 GK is better described by the dineutron model with $V_{0y} = -14$ MeV, reproducing best the "bulk" of the three-body SF.

If we perform the rate calculations starting with the asymptotic expression for the SF (10) then the rate is given by

$$\langle\sigma_{2n,\gamma}\,v\rangle \sim T\left[1 + 12(E_b/T) + 60(E_b/T)^2 + \ldots\right]. \tag{12}$$

This asymptotic expression (shown by the green dashed curve in Fig. 8) is very precise up to $T \sim 0.1$ GK and at $T \sim 0.6$ GK the difference from the three-body SF is just a factor of 2. This emphasizes the importance of a correct description of the SF low-energy asymptotics.

Finalizing the discussion here, the phenomenological recipe for using the dineutron model seems very simple:

(i) If there is no experimental information at all, then it is very reasonable to make the rate estimates with $V_y \equiv 0$. As we have seen above, in the case of ^{6}He the overall agreement in a broad temperature range is also very reasonable.
(ii) If there is experimental information about E1 strength function, parameters of the dineutron model can be fitted to the experimental SF profile. In that case we have nearly perfect description of the rate at $T > 0.7 - 1.0$ GK. At $T \to 0$ the dineutron model does not guarantee precise asymptotic behavior, but the mismatch is not severe.
(iii) Despite the uncertainties of the dineutron model it immediately provides the results which is much closer to the highly accurate three-body calculation results than any result obtained in this field before, see Fig. 8 and discussion of the next Section. In that sense it is very strong phenomenological tool.

5. Comparison with previous results

The calculations of the astrophysical radiative capture rate for the ^{4}He+n+$n \to {}^6$He+γ reaction are given in a number of papers [7–12]. The results of the papers [7–9] are based on different quasiclassical two-step approximations. So, maybe, it is not surprising that they are highly incompatible with each other and with results of this work.

More attention needs to be paid to the results of the three-body model [10–12], which, in principle, should be consistent with the results of this work. There are two issues.
(i) All three results [10–12] are declared to be based on the same E1 SF from paper [10]. However, different rate values can be found in papers [10–12], see Fig. 8. We have no understanding of this fact.
(ii) It was discussed in Ref. [13] that the E1 SF from [10] has some kind of suspicious enhancement of the low-energy behavior, which is not reproduced in the other three-body approaches (see Fig. 9 of this work, Fig. 14 in Ref. [13], and also Refs. [21,22]).

We attempted to reproduce the low-energy behavior of the E1 SF [10] in the dynamical dineutron model. That was found to be very difficult. Evidently, the low-energy enhancement of the SF requires the reduction of the centrifugal barrier in the Y channel (for E1 transition the "dineutron" cluster should be in $l_y = 1$ relatively α-core). It can be seen in Fig. 9 that the SF, which is pretty close to [10], can be obtained in the dineutron model. However, this requires an unrealistic potential in Y channel: here we use Gaussian potential with extremely large radius of $Y_0 = 6$ fm, which in our opinion has no reasonable justification. And even so, if we look in Fig. 7 it can be found that still it does not help to reproduce the correct asymptotic low-energy behavior of the E1 SF. Even more extreme potential, with $Y_0 = 8$ fm, is required to reproduce the behavior of SF from [10] down to $E_T \sim 0.3$ MeV and for lower energies the dineutron SF turns to expected $\sim E_T^3$ trend. So, in the log-scale it can be seen that the low-energy SF of [10] has no chance to be reconciled with ours.

The rate calculated in [10] overlaps with our three-body result in a broad temperature range (and it is drastically smaller for $T <$ 0.5 GK). We think that this contradicts SF behavior. The dineutron SF with $Y_0 = 6$ fm approximates SF [10] well: it is *smaller or equal* to SF [10] in the whole energy range, see Fig. 9. However, the rate computed with this dineutron SF is *larger* than the rate from [10] in the whole temperature range, see Fig. 8.

6. Conclusion

The convergence of the SDM (E1) strength function for ^{6}He becomes slower with decreasing decay energies. Large-basis (with $K_{\max} = 101$) calculations allowed to obtain fully converged SF values down to energies as low as 60-80 keV. For the lower energies (e.g., as small as 1 keV) it was shown that the extrapolation scheme allows to obtain reliable SF values.

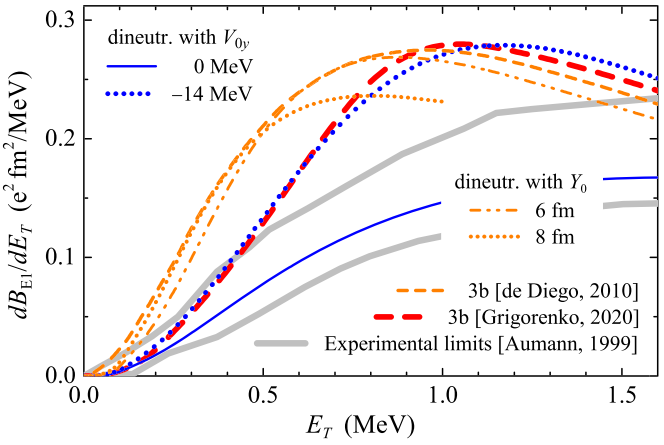

Fig. 9. Comparison of the E1 low-energy strength functions calculated in our full three-body model (Grigorenko, 2020: [13]), in different dineutron model settings, in paper (de Diego, 2010: [10]) with experimental data of Ref. (Aumann, 1999: [23]).

It was demonstrated that the low-energy E1 SF in ^{6}He case is strongly affected by the virtual state in the spin-singlet n-n channel. For that reason a very reliable approximation for the low-energy E1 SF can be obtained in a dynamical dineutron model. Within the dineutron approximation the three-body dynamics is reduced to a kind of factorized two-body semisequential dynamics. As a result, the three-body Green's function in the dineutron approximation has a compact analytical form, allowing exact semi-analytical calculations. This is an important result in several ways:
(i) The dineutron model provides a simple semianalytical cross check and reliable shortcut for the bulky three-body calculations for the low-energy three-body (namely, two-neutron) radiative capture reactions.
(ii) Important *qualitative difference* between two-proton and two-neutron radiative captures is elucidated, see Fig. 5. In the case of the low-energy two-proton capture the dynamics is also factorized to two-body semisequential dynamics, but in the "Y" Jacobi system, which allows to take into account the low-lying resonances in the core+p channel. The diproton correlation does not play important role in the low-energy region.
(iii) The effective low-energy reduction of the three-body dynamics to dynamics of dineutron emission may be seen as very intuitive and even trivial result. However, without bulky three-body calculations we would never be sure at what level of accuracy this approach really works. Now, the semi-analytical dineutron model, supported by our high-precision three-body calculations, reliably predicts the low-energy behavior of the strength function and capture rates and, thus, provides reliable extrapolation of experimental data measured at sufficiently high energies.

All the previous results [7–12] for the ^{4}He+n+$n \to {}^6$He+γ astrophysical radiative capture rate are highly inconsistent with each other and with the results of this work. For calculations [10–12] the origin of important problems can be identified as inconsistent treatment of the low-energy region of the E1 SF. Thus, our results emphasize the importance of the accurate treatment of few-body dynamics for consistent determination of the low-temperature parts of the astrophysical three-body capture rates.

Declaration of competing interest

The authors declare that they have no known competing financial interests or personal relationships that could have appeared to influence the work reported in this paper.

Acknowledgements

LVG and NBS were supported in part by the Russian Science Foundation grant No. 17-12-01367.

References

[1] W. Fowler, G. Caughlan, B. Zimmerman, Annu. Rev. Astron. Astrophys. 5 (1967) 525.
[2] C. Angulo, M. Arnould, M. Rayet, P. Descouvemont, D. Baye, C. Leclercq-Willain, A. Coc, S. Barhoumi, P. Aguer, C. Rolfs, R. Kunz, J. Hammer, A. Mayer, T. Paradellis, S. Kossionides, C. Chronidou, K. Spyrou, S. del'Innocenti, G. Fiorentini, B. Ricci, S. Zavatarelli, C. Providencia, H. Wolters, J. Soares, C. Grama, J. Rahighi, A. Shotter, M.L. Rachti, Nucl. Phys. A 656 (1999) 3–183.
[3] L.V. Grigorenko, M.V. Zhukov, Phys. Rev. C 72 (2005) 015803.
[4] L. Grigorenko, K. Langanke, N. Shul'gina, M. Zhukov, Phys. Lett. B 641 (3) (2006) 254–259.
[5] L.V. Grigorenko, M.V. Zhukov, Phys. Rev. C 76 (2007) 014009.
[6] Y.L. Parfenova, L.V. Grigorenko, I.A. Egorova, N.B. Shulgina, J.S. Vaagen, M.V. Zhukov, Phys. Rev. C 98 (2018) 034608.
[7] V.D. Efros, W. Balogh, H. Herndl, R. Hofinger, H. Oberhummer, Z. Phys. Hadrons Nucl. 355 (1996) 101–105.
[8] A. Bartlett, J. Görres, G.J. Mathews, K. Otsuki, M. Wiescher, D. Frekers, A. Mengoni, J. Tostevin, Phys. Rev. C 74 (2006) 015802.
[9] J. Görres, H. Herndl, I.J. Thompson, M. Wiescher, Phys. Rev. C 52 (1995) 2231–2235.
[10] R. de Diego, E. Garrido, D. Fedorov, A. Jensen, Europhys. Lett. 90 (2010) 52001.
[11] R. de Diego, E. Garrido, D.V. Fedorov, A.S. Jensen, Few-Body Syst. 50 (2011) 331.
[12] R. de Diego, E. Garrido, D.V. Fedorov, A.S. Jensen, Eur. Phys. J. A 50 (2014) 93.
[13] L.V. Grigorenko, N.B. Shulgina, M.V. Zhukov, arXiv:2003.10701.
[14] T. Schneider, Phys. Lett. B 40 (4) (1972) 439–442.
[15] L.V. Grigorenko, M.V. Zhukov, Phys. Rev. C 76 (2007) 014008.
[16] L.V. Grigorenko, T.D. Wiser, K. Mercurio, R.J. Charity, R. Shane, L.G. Sobotka, J.M. Elson, A.H. Wuosmaa, A. Banu, M. McCleskey, L. Trache, R.E. Tribble, M.V. Zhukov, Phys. Rev. C 80 (2009) 034602.
[17] K.W. Brown, R.J. Charity, L.G. Sobotka, Z. Chajecki, L.V. Grigorenko, I.A. Egorova, Y.L. Parfenova, M.V. Zhukov, S. Bedoor, W.W. Buhro, J.M. Elson, W.G. Lynch, J. Manfredi, D.G. McNeel, W. Reviol, R. Shane, R.H. Showalter, M.B. Tsang, J.R. Winkelbauer, A.H. Wuosmaa, Phys. Rev. Lett. 113 (2014) 232501.
[18] K.W. Brown, R.J. Charity, L.G. Sobotka, L.V. Grigorenko, T.A. Golubkova, S. Bedoor, W.W. Buhro, Z. Chajecki, J.M. Elson, W.G. Lynch, J. Manfredi, D.G. McNeel, W. Reviol, R. Shane, R.H. Showalter, M.B. Tsang, J.R. Winkelbauer, A.H. Wuosmaa, Phys. Rev. C 92 (2015) 034329.
[19] L.V. Grigorenko, T.A. Golubkova, J.S. Vaagen, M.V. Zhukov, Phys. Rev. C 95 (2017) 021601.
[20] L.V. Grigorenko, J.S. Vaagen, M.V. Zhukov, Phys. Rev. C 97 (2018) 034605.
[21] A. Cobis, D. Fedorov, A. Jensen, Phys. Rev. Lett. 79 (1997) 2411.
[22] T. Myo, K. Kato, S. Aoyama, K. Ikeda, Phys. Rev. C 63 (2001) 054313.
[23] T. Aumann, D. Aleksandrov, L. Axelsson, T. Baumann, M.J.G. Borge, L.V. Chulkov, J. Cub, W. Dostal, B. Eberlein, T.W. Elze, H. Emling, H. Geissel, V.Z. Goldberg, M. Golovkov, A. Grünschloß, M. Hellström, K. Hencken, J. Holeczek, R. Holzmann, B. Jonson, A.A. Korshenninikov, J.V. Kratz, G. Kraus, R. Kulessa, Y. Leifels, A. Leistenschneider, T. Leth, I. Mukha, G. Münzenberg, F. Nickel, T. Nilsson, G. Nyman, B. Petersen, M. Pfützner, A. Richter, K. Riisager, C. Scheidenberger, G. Schrieder, W. Schwab, H. Simon, M.H. Smedberg, M. Steiner, J. Stroth, A. Surowiec, T. Suzuki, O. Tengblad, M.V. Zhukov, Phys. Rev. C 59 (1999) 1252–1262.